PHYSICAL REVIEW D, VOLUME 58, 084004

Stability of a dilatonic black hole with a Gauss-Bonnet term

Takashi Torii*
Department of Physics, Tokyo Institute of Technology, Meguro-ku, Tokyo 152, Japan

Kei-ichi Maeda†
Department of Physics, Waseda University, Shinjuku-ku, Tokyo 169, Japan

(Received 19 February 1998; published 31 August 1998)

We investigate the stability of black hole solutions in an effective theory derived from a superstring model, which includes a dilaton field and the Gauss-Bonnet term. The critical solution, below which mass no static solution exists, divides a family of solutions in the mass-entropy diagram into two. The upper branch approaches the Schwarzschild solution in the large mass limit, while the lower branch ends up with a singular solution which has a naked singularity. In order to investigate the stability of black hole solutions, we adopt two methods. The first one is catastrophe theory, with which we discuss the stability of non-Abelian black holes in general relativity. The present system is classified as a fold catastrophe, which is the simplest case. Following catastrophe theory, if we regard entropy and mass as the potential and the control parameter, respectively, we find the lower branch is more unstable than the upper branch. To confirm this, we study the second method, which is a linear perturbation analysis. We find an unstable mode only for the solutions in the lower branch. Hence, our investigation presents one example that catastrophe theory is also applicable for a generalized theory of gravity. [S0556-2821(98)02118-3]

PACS number(s): 04.50.+h, 04.70.Bw, 04.70.Dy, 11.15.−q

I. INTRODUCTION

A black hole is one of the most interesting stellar objects which reflects general relativistic effects. Investigation of black holes includes many topics and it would unveil a new physics. Simultaneously, however, many unsolved problems have come out. For example, we now have several conjectures or problems such as the black hole no-hair conjecture, the information loss problem, a cosmological remnant after black hole evaporation. As one of the attempts to investigate these problems, several researchers have discussed black hole solutions in effective string theories.

The first study of such a black hole was made in the Einstein-Maxwell-dilaton system [1,2]. They derived new black hole solutions with a dilaton hair in spherically symmetric static spacetime. It is classified as a secondary hair because it is not independent of electromagnetic charge. The effect of the next leading order term in the inverse string tension α', in particular higher curvature term, was studied by many authors [3–6]. Recently, black hole solutions in the system including the dilaton field, the gauge field, and the Gauss-Bonnet term were solved numerically [7–9]. These solutions, which we call dilatonic black holes with Gauss-Bonnet term, have the following interesting properties.

(1) There is a critical solution, below which mass no static solution exists.

(2) There is a singular solution, which has a naked singularity.

(3) For the neutral and the electrically charged black holes, the critical solution is not the same as the singular one, while those two solutions coincide for the magnetically charged and the ''colored'' black holes.

(4) The entropy takes the minimum value at the critical solution, and a cusp structure appears in the mass-entropy diagram for neutral and electrically charged black holes. On the other hand, no cusp structure appears for magnetically charged and ''colored'' black holes.

(5) The black hole temperature is always finite and heat capacity is always negative for any type of black hole.

Note that in the above system, the black hole can support a dilaton hair without an electromagnetic or other gauge charge, while the ''no scalar-hair theorem'' guarantees that there is no black hole solution with a dilaton hair under the appropriate conditions in asymptotically flat spacetime in general relativity [10–12]. This is because the existence of nontrivial dilaton hair is due to the Gauss-Bonnet term. Then, this hair can also be classified as a secondary hair [7]. Hence, there is no analogue of the ''no scalar-hair'' theorem in the present model. However if dilatonic black holes with the Gauss-Bonnet term are unstable, such a scalar hair has no meaning physically. Hence, stability analysis of new solutions is indispensable.

The fact that black hole mass is bounded below is also important because such a critical solution can be a candidate of cosmological remnant and it may solve the information loss problem. However as the temperature is always finite, evaporation does not stop even at the critical solution. Hence a further problem appears: what state does such a black hole develop into though evaporation? This has been an open question. If a singular solution forms generically, it can be a counterexample to the cosmic censorship conjecture. One of the methods to investigate this problem is the stability analysis. If the singular solution is unstable, the naked singularity seems not to be formed from the regular initial data generically. With these motivations, we investigate whether or not dilatonic black holes with the Gauss-Bonnet term are stable.

*Electronic address: torii@th.phys.titech.ac.jp
†Electronic address: maeda@mn.waseda.ac.jp

Previously, we showed that catastrophe theory is useful for discussing the stability of black hole solutions with non-Abelian matter fields in general relativity [13,14]. Although in general relativity, there is a close relation between catastrophe theory and linear perturbation analysis [15], we are not sure whether a similar discussion holds in generalized theories of gravity. In this paper, we will give one example that catastrophe theory is applicable for the model including the Gauss-Bonnet term [16].

This paper is organized as follows. We outline the model and derive static solutions in Sec. II. In Sec. III we investigate the stability by using both catastrophe theory and linear perturbation analysis. Section IV includes discussions and some remarks.

II. DILATONIC BLACK HOLE WITH GAUSS-BONNET TERM

We only consider the bosonic part of effective field theory of a heterotic string theory [17]. The action is described as follows

$$S=\int d^4x\sqrt{-g}\left(\frac{1}{2\kappa^2}R-\frac{1}{2\kappa^2}(\nabla\phi)^2+f(\phi)(R_{GB}^2-F^2)\right). \tag{1}$$

This includes only tree level in expansion of inverse string tension α'. Here $\kappa^2=8\pi G$ and R_{GB}^2 is the Gauss-Bonnet term, i.e.,

$$R_{GB}^2=R_{\mu\nu\rho\sigma}R^{\mu\nu\rho\sigma}-4R_{\mu\nu}R^{\mu\nu}+R^2. \tag{2}$$

The function $f(\phi)$ is defined as

$$f(\phi)=\frac{\alpha'}{16\kappa^2}\mathrm{e}^{-\gamma\phi}, \tag{3}$$

where $\gamma=\sqrt{2}$ is the coupling constant of dilaton field ϕ and g is regarded as a gauge coupling constant. We neglect the rank three antisymmetric tensor field, which vanishes in the spherically symmetric case. Furthermore, we assume no gauge field and focus only on the neutral case with the Gauss-Bonnet term just for simplicity.

Varying the action (1) by the metric and the dilaton field, we obtain the basic equations of the gravitational field

$$\begin{aligned}G_{\mu\nu}=&-\frac{1}{2}g_{\mu\nu}(\nabla\phi)^2+\nabla_\mu\nabla_\nu\phi+\kappa^2 f(R_{GB}^2 g_{\mu\nu}-4RR_{\mu\nu}\\&+8R_\mu{}^\lambda R_{\nu\lambda}+8R_{\mu\rho\nu\sigma}R^{\rho\sigma}-4R_{\rho\sigma\lambda\mu}R^{\rho\sigma\lambda}{}_\nu)\\&+4\kappa^2(\nabla^\rho\nabla^\sigma f)(g_{\mu\rho}g_{\nu\sigma}R+2g_{\rho\sigma}G_{\mu\nu}\\&-4g_{\nu\sigma}R_{\mu\rho}+2g_{\mu\nu}R_{\rho\sigma}+2R_{\rho\mu\nu\sigma}),\end{aligned} \tag{4}$$

and of the dilaton field

$$\Box\phi+\frac{\partial f}{\partial\phi}R_{GB}^2=0. \tag{5}$$

The coupling between the Gauss-Bonnet term and the dilaton field plays a crucial role. Without this coupling, the Gauss-Bonnet term becomes totally divergent and there will not exist any nontrivial black hole solution in the static spherically symmetric spacetime because such a solution is forbidden by the no scalar-hair theorem.

In this paper, we consider a spherically symmetric spacetime. Hence, we adopt the following form of the metric,

$$ds^2=-e^{2\Phi(t,r)}dt^2+e^{2\Lambda(t,r)}dr^2+r^2(d\theta^2+\sin^2\theta d\varphi^2). \tag{6}$$

We also use the lapse function δ and the mass function m defined as

$$\delta(t,r)\equiv-(\Phi+\Lambda), \tag{7}$$

$$Gm(t,r)\equiv r(1-e^{-2\Lambda}), \tag{8}$$

respectively. Then the metric is rewritten with these functions as

$$\begin{aligned}ds^2=&-\left(1-\frac{2Gm(t,r)}{r}\right)^{-1}e^{-2\delta(t,r)}dt^2\\&+\left(1-\frac{2Gm(t,r)}{r}\right)dr^2+r^2(d\theta^2+\sin^2\theta d\varphi^2).\end{aligned} \tag{9}$$

By using these *Ansätze*, we write down the field equations explicitly. The nontrivial equations of Eq. (4) are

$$\Lambda'\left(1+\frac{4}{\tilde{r}}\tilde{f}'(1-3e^{-2\Lambda})\right)=\frac{\tilde{r}}{4}(\phi'^2+e^{2\Lambda-2\Phi}\dot{\phi}^2)+\frac{1}{2\tilde{r}}(1-e^{2\Lambda})+\frac{4}{\tilde{r}}(1-e^{-2\Lambda})(\tilde{f}''-e^{2\Lambda-2\Phi}\dot{\Lambda}\dot{\tilde{f}}), \tag{10}$$

$$\Phi'\left(1+\frac{4}{\tilde{r}}\tilde{f}'(1-3e^{-2\Lambda})\right)=\frac{\tilde{r}}{4}(\phi'^2+e^{2\Lambda-2\Phi}\dot{\phi}^2)-\frac{1}{2\tilde{r}}(1-e^{2\Lambda})+\frac{4}{\tilde{r}}(1-e^{-2\Lambda})e^{2\Lambda-2\Phi}(\ddot{\tilde{f}}-\dot{\Phi}\dot{\tilde{f}}), \tag{11}$$

$$\dot{\Lambda}\left(1+\frac{4}{\tilde{r}}\tilde{f}'(1-3e^{-2\Lambda})\right)=\frac{\tilde{r}}{4}(1-e^{2\Lambda})(\dot{\tilde{f}}'-\Phi'\dot{\tilde{f}})+\frac{\tilde{r}}{2}\dot{\phi}\phi', \tag{12}$$

$$\Phi''+\left(\Phi'+\frac{1}{\tilde{r}}\right)(\Phi'-\Lambda')-e^{2\Lambda-2\Phi}[\ddot{\Lambda}+\dot{\Lambda}(\dot{\Lambda}-\dot{\Phi})]+\frac{1}{2}(\phi'^2-e^{2\Lambda-2\Phi}\dot{\phi}^2)-\frac{16}{\tilde{r}}\{e^{-2\Lambda}[(\tilde{f}'\Phi')'+\tilde{f}'\Phi'(\Phi'-3\Lambda')]$$
$$+e^{-2\Phi}[\tilde{f}'\dot{\Lambda}(\dot{\Lambda}+\dot{\phi})-\tilde{f}'\ddot{\Lambda}+\dot{\tilde{f}}(\Phi'\dot{\Lambda}-\dot{\phi}\Lambda')-2\dot{\Lambda}\dot{\tilde{f}}'+\Lambda'\ddot{\tilde{f}}]\}=0. \tag{13}$$

Here we have used the dimensionless variables; $\tilde{r}=r/\sqrt{\alpha'}$, $\tilde{t}=t/\sqrt{\alpha'}$, and $\tilde{f}=\kappa^2 f/\alpha'$. A dot and a prime denote derivative with respect to $\tilde{t}$ and $\tilde{r}$, respectively. The equation of the dilaton field is described as

$$\phi''+\left(\Phi'-\Lambda'+\frac{2}{\tilde{r}}\right)-e^{2\Lambda-2\Phi}[\ddot{\phi}+(\dot{\Lambda}-\dot{\Phi})\dot{\phi}]=\frac{\partial\tilde{f}}{\partial\phi}\frac{8}{\tilde{r}^2}\{2e^{-2\Lambda}\Phi'\Lambda'-2e^{-2\Phi}\dot{\Lambda}^2+(1-e^{2\Lambda})[\Phi''+\Phi'(\Phi'-\Lambda')]$$
$$-(1-e^{2\Lambda})e^{2\Lambda-2\Phi}[\ddot{\Lambda}+\dot{\Lambda}(\dot{\Lambda}-\dot{\Phi})]\}. \tag{14}$$

The right-hand side comes from the coupling with the Gauss-Bonnet term. Since these equations are not independent, we use Eq. (13) as an error check in our numerical calculation.

Dropping the terms which include time derivative in the field equations (10)–(14), we find the dilatonic black hole solution with the Gauss-Bonnet term in the static spacetime. We, of course, need the boundary and regularity conditions of metric functions and the dilaton field as follows. At infinity, the spacetime approaches the flat one, i.e., as $r\to\infty$

$$\Phi(r)\to 0, \tag{15}$$

$$\Lambda(r)\to 0, \tag{16}$$

or

$$m(r)\to M=\text{finite}, \tag{17}$$

$$\delta(r)\to 0. \tag{18}$$

The constant M is the mass of a black hole. We assume the existence of a regular event horizon r_H, i.e.,

$$2Gm_H=r_H, \tag{19}$$

$$\delta_H<\infty. \tag{20}$$

Here the variables with a subscript H denote those values at the event horizon. Furthermore, we assume the nonexistence of a singularity outside the event horizon, i.e., for $r>r_H$,

$$2Gm(r)<r. \tag{21}$$

From the boundary conditions (17) and (18), the dilaton field should approach a constant value ϕ_∞. It has been already fixed in our universe. In principle, we can estimate ϕ_∞ by discussing the gauge coupling constant. As the spacetime approaches flat Minkowski space in the far region from the black hole, Maxwell theory in the Minkowski spacetime must be recovered. Comparing the Lagrangian (1) with Lagrangian of the electromagnetic field, we find the following relation,

$$\frac{\alpha'}{16\kappa^2}e^{-\gamma\phi_\infty}=\frac{1}{16\pi g^2}. \tag{22}$$

The gauge coupling constant at the low-energy scale is determined by experiments as $1/g^2\sim O(10^2)$. If we know the value of the inverse string tension α' and if the renormalization effect does not change its value so much, we can estimate ϕ_∞ from Eq. (22). However there is no way to fix α' even if a string theory and its low-energy limit are relevant to our universe. We just expect that it must be the Planck scale. Here we assume $\phi_\infty=0$. If we are interested in a different boundary condition such as $\phi\to\phi_\infty^*\neq 0$, we can always have such a boundary condition without further calculation because the constant difference is absorbed in the coordinates by rescaling. That is, introducing $\overline{\phi}\equiv\phi-\phi_\infty^*$, and rescaling the variables as $\overline{r}=e^{-\gamma\phi_\infty^*}\tilde{r}$, $\overline{t}=e^{-\gamma\phi_\infty^*}\tilde{t}$, and $\overline{m}=e^{-\gamma\phi_\infty^*}\tilde{m}$, we recover our boundary condition.

The equation of the dilaton field is singular on the event horizon. In order to guarantee to find a regular solution at the event horizon, we expand variables around the event horizon by power series of $\epsilon\equiv(\tilde{r}-\tilde{r}_H)/\tilde{r}_H$ as

$$\tilde{m}(r)=\tilde{m}_H+\tilde{m}_H^{(1)}\epsilon+\frac{1}{2}\tilde{m}_H^{(2)}\epsilon^2+\cdots+\frac{1}{n!}\tilde{m}_H^{(n)}\epsilon^n+\cdots, \tag{23}$$

$$\delta(r)=\delta_H+\delta_H^{(1)}\epsilon+\frac{1}{2}\delta_H^{(2)}\epsilon^2+\cdots+\frac{1}{n!}\delta_H^{(n)}\epsilon^n+\cdots, \tag{24}$$

$$\phi(r)=\phi_H+\phi_H^{(1)}\epsilon+\frac{1}{2}\phi_H^{(2)}\epsilon^2+\cdots+\frac{1}{n!}\phi_H^{(n)}\epsilon^n+\cdots. \tag{25}$$

Substituting them into field equations (10), (11), and (14), we obtain the coefficients $\tilde{m}_H^{(n)}$, $\delta_H^{(n)}$, $\phi_H^{(n)}$ $(n=1,2,\dots)$ order by order. From the zeroth-order equations of ϵ, we find the following relation for the dilaton field on the event horizon:

$$\phi_H'^2-\frac{\phi_H'}{c_0\gamma}+3=0, \tag{26}$$

where $c_0=e^{-\gamma\phi_H}/4\tilde{r}_H^2$. This quadratic equation has two roots as

$$\phi'_{H\pm} = \frac{1 \pm \sqrt{1-12c_0^2\gamma^2}}{2c_0\gamma}. \tag{27}$$

By the reality condition of $\phi'_{H\pm}$, ϕ_H is restricted as

$$\phi_H \geqslant -\frac{1}{2\gamma}\ln\left(\frac{4\tilde{r}_H^4}{3\gamma^2}\right), \tag{28}$$

for each horizon radius. In the numerical calculation, we find black hole solutions with a regular horizon only when we choose the minus sign in the boundary condition (27).

From the second-order equation

$$\phi''_H = \frac{E}{D}. \tag{29}$$

D and E are very complicated functions of $\tilde{m}_H$, δ_H, and ϕ_H. It must be noted that if we take the minimum value of ϕ_H, i.e., $\phi_H = -\ln(4\tilde{r}_H^4/3\gamma^2)/2\gamma$, the denominator D vanishes, while the numerator E remains finite. Hence ϕ''_H diverges. Furthermore, we have checked that a scalar invariant $I \equiv R_{\mu\nu\rho\sigma}R^{\mu\nu\rho\sigma}$ also diverges, which means that a naked singularity will appear on the ''horizon'' $r = r_H$.

We integrate the static field equations from the event horizon with the above boundary conditions. The properties of dilatonic black holes with Gauss-Bonnet term are discussed in detail in Refs. [7–9]. Figure 1 is the M-r_H diagram. We find an end point S which has the minimum horizon radius. At this point S, $\phi_H = -\ln(4\tilde{r}_H^4/3\gamma^2)/2\gamma$, then a naked singularity appears at $r = r_H$. It is no longer a black hole. We call this point S, the singular point. We also find another important point C, which has the minimum mass. At this point, the solution curve turns around. We call this point C, the critical point. The existence of the critical point plays an important role in the stability analysis using catastrophe theory.

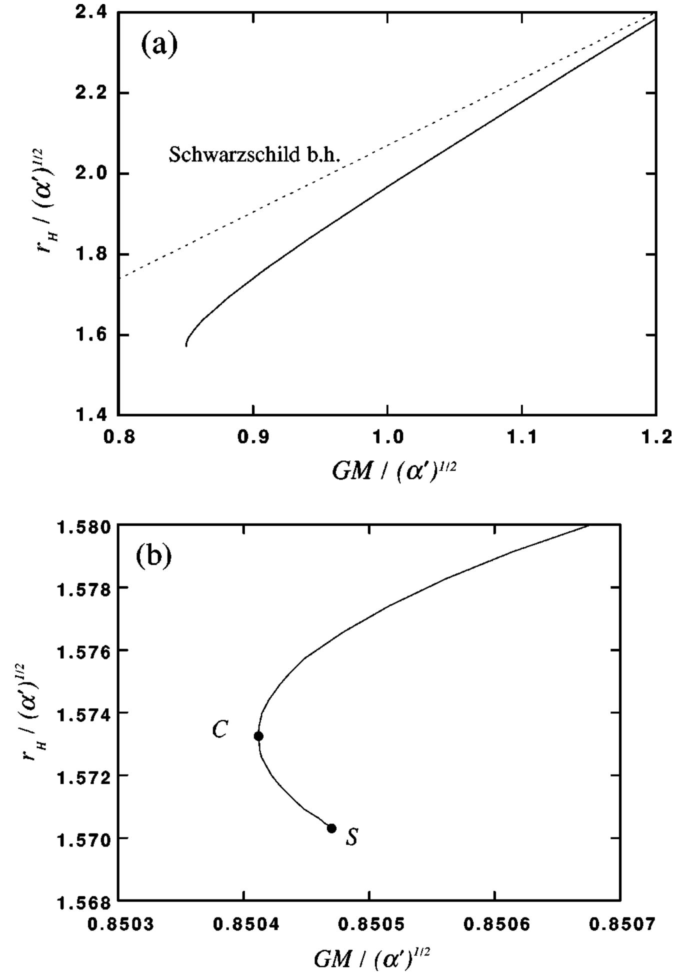

FIG. 1. (a) The mass-horizon radius diagram for the dilatonic black holes with Gauss-Bonnet term. There is an end point S, where a naked singularity appears. We also plot the Schwarzschild black hole for comparison. In the large mass limit, the dilatonic black hole approaches the Schwarzschild black hole. (b) is a magnification around the singular point S. We find the critical point C, below which no solution exists.

III. STABILITY ANALYSIS

Now we discuss a stability of the dilatonic black hole with the Gauss-Bonnet term. The stability of the solution is one of the most important properties. In particular, our analysis of the static solution shows a possibility that a naked singularity may appear. Hence, we will analyze the stability around the singular point and the critical point in detail. In this paper, we adopt two methods.

A. Catastrophe theory

Catastrophe theory is a mathematical tool to investigate a variety of changes of states in nature. Especially, it is useful when we treat an unexpected and discontinuous change of states. It is widely applied in various research fields, for example the structural stability, the crystal lattice, biology, embryology, and astrophysics. Previously, we showed that it is also applicable to the stability analysis of various types of non-Abelian black holes in general relativity [13,14].

In order to apply catastrophe theory, first we have to define several catastrophe variables of the system. First group is the control parameter, with which we can control the system. Here we choose the mass of a black hole as the control parameter, since we can change the black hole state by throwing a mass into it. The second group is the state variables, which describe a state of the system. In the non-Abelian black hole case, we adopted the field strength of the gauge field on the horizon. However in the present system no gauge field exists. Hence, we choose the dilaton field ϕ_H as the state variable instead of the gauge field. The third group is a potential function, whose extremum should correspond to equilibrium states. In general relativity, we adopted the entropy as the potential function, which is expressed by one quarter of the area of the event horizon. The increase of the area is guaranteed by the area theorem, i.e., the second law of the black hole thermodynamics. In generalized theories of gravity, however, it is not the case. In fact, Oppenheimer-Schneider collapse in Brans-Dicke theory reveals a decrease of the area [18]. Nevertheless, the entropy defined by Kang does not decrease at any stage in their simulation. Furthermore, Jacobson and Kang showed that the second law of black hole thermodynamics is still valid in the following restricted model,

$$S=\int d^4x\sqrt{-g}[f(R)+\mathcal{L}_{matter}], \tag{30}$$

with null energy condition [19]. $f(R)$ is a polynomial of the Ricci scalar. The entropy defined above has been extended into a more generic model by Iyer and Wald [20]. Hence, as the potential function, we adopt the entropy defined by Iyer and Wald as in general relativity.

This definition of entropy has the following desirable properties. It can be defined in a covariant way in any diffeomorphism invariant theory and it obeys the first law of black hole thermodynamics for an arbitrary perturbation of a stationary black hole. We present its expression in the present model. The explicit form is obtained by

$$S=-2\pi\int_\Sigma E_R^{\mu\nu\rho\sigma}\epsilon_{\mu\nu}\epsilon_{\rho\sigma}, \tag{31}$$

where Σ is the bifurcation horizon 2-surface and $\epsilon_{\mu\nu}$ denotes the volume element binormal to Σ. $E_R^{\mu\nu\rho\sigma}$ is defined by

$$E_R^{\mu\nu\rho\sigma}=\frac{\partial\mathcal{L}}{\partial R_{\mu\nu\rho\sigma}}, \tag{32}$$

where $\mathcal{L}$ is the Lagrangian density. Then in our model, we find

$$S=\frac{A_H}{4G}\left(1+\frac{\alpha'}{2r_H^2}e^{-\gamma\phi_H}\right), \tag{33}$$

where A_H is the area of the event horizon. The second term in the round bracket is the correction from the Gauss-Bonnet term.

In order to investigate whether the stability change occurs, we draw Whitney surface, which is a solution surface drawn in the space of control parameters p_i, state variables x_j, and a potential function V. A schematic diagram with $i=j=1$ is given in Fig. 2. When we fix the control parameters, extrema of the Whitney surface give equilibrium solutions. When the extremum is the minimum, the solution is stable, while if it is the maximum point, the solution is found out to be unstable, when we adopt the usual definition of a potential function like the energy of a system. Hence in Fig. 2 the branch AC is more stable than the branch BC. The projection of equilibrium solutions onto the p-V plane gives a cusp structure C, which corresponds to the infection point of the three-dimensional figure. As a result, stability change occurs at the cusp point C on the p-V plane.

As this example, if the stability of solutions changes for a certain parameter, its sign appears on the diagram of control parameters versus a potential function. The diagram in the present model is shown in Fig. 3. In order to show the structure at the critical point clearly, we depict $S^*(M)=S(M)-S_0(M)$, where $S_0(M)$ is a linear function of M passing through an appropriate point A in the upper branch and the end point S. We can find a cusp structure at the critical point C and it is the characteristic sign of a stability change. From this figure, we conclude that solutions in the lower branch are more unstable than those in the upper branch, since the higher entropy means the more stable. Usually, the minimum and the maximum of the potential function correspond to

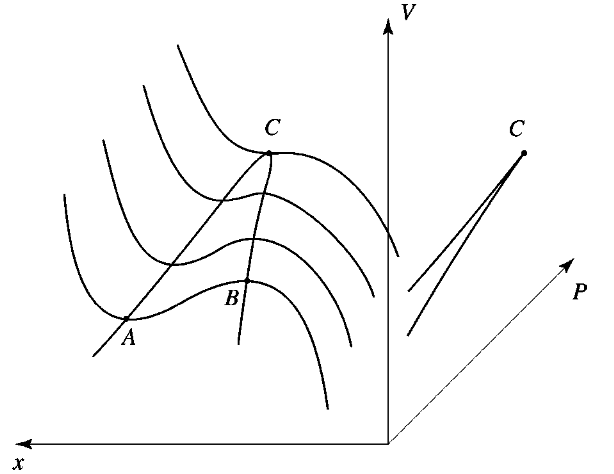

FIG. 2. The Whitney surface in the control parameter p, the state variable x, and the potential function V space. Extrema of this surface for the fixed control parameter are denoted by dotted line ACB, which corresponds to the family of static solutions of the system. The minimum line AC and the maximum line BC are stable and unstable solutions, respectively. Stability change occurs at the inflection point C. We also plot the projection of the static solutions onto the p-x plane and find a cusp structure at the point C. This is a characteristic sign that the catastrophe occurs.

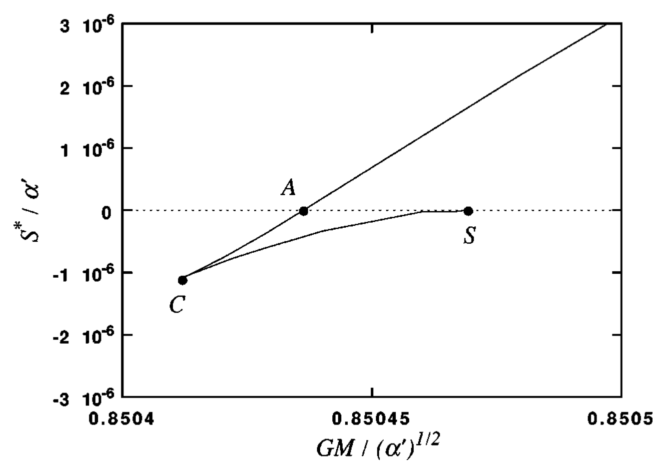

FIG. 3. We plot the entropy for the dilatonic black holes with Gauss-Bonnet term. This is the magnification around the critical point and the singular point. In order to show the structure at the critical point clearly, we depict $S^*(M)=S(M)-S_0(M)$, where $S_0(M)$ is a linear function of M passing through an appropriate point A in the upper branch and the end point S. Hence, the absolute value has no meaning. We can find a cusp structure, which separates the family of solutions into two branches, at the critical point C. This means that the stability change occurs at the critical point and solutions of the upper branch AC are stable, while the lower branch SC is unstable.

stable and unstable solutions, respectively. However, since we adopted the entropy as a potential function, the correspondence turns out to be opposite.

Catastrophe theory shows only a relative stability among several families of solutions. We cannot predict the absolute stability of solutions. However we expect that the upper branch in Fig. 3 is absolutely stable from the following two reasons. There is no solution except for those obtained above, hence, if the solutions of the upper branch are unstable, there is no stable static solution and we must give up staticity or spherical symmetry. Next, in the limit of $r_H \to \infty$, the effect of the Gauss-Bonnet term vanishes and our system approaches general relativity with a massless scalar field. From the no hair theorem in general relativity, the solutions of the upper branch approach to the Schwarzschild black hole, which is stable in general relativity.

Next we investigate what type of catastrophe, the dilatonic black hole with Gauss-Bonnet term is classified into. The first step is drawing the equilibrium space M_S, which consists of extrema of the potential function in the space of control parameters and state variables. Then we project the equilibrium space onto a control parameter space, which is called the control plane, by a catastrophe map χ_S. There may exist singular points on equilibrium space, where the Jacobian of the mapping χ_S vanishes. The image of the set of singular points is the bifurcation set B_S. If such singular points exist, the number of solutions with the same control parameter changes beyond the bifurcation set B_S, and then the stability also changes there. Hence, by looking at this bifurcation set, we can classify our model into elementary catastrophes.

Until now, we have fixed the value of the dilaton field at infinity as $\phi_\infty = 0$ because it is related to the physical constant. However we are now interested in the elementary catastrophe of the present system (10)–(14) from the mathematical point of view. For this purpose, we have to vary all possible parameters. In the present model, we have two control parameters. Hence, in addition to mass *M*, we adopt ϕ_∞ as the second control parameter, although ϕ_∞ is a different type of control parameter from the black hole mass *M* in the following sense. We can control *M* by putting matter into the black hole, on the other hand, we cannot change ϕ_∞ by any physical process because it needs infinite energy. We plot the equilibrium space and the bifurcation set of dilatonic black holes with Gauss-Bonnet term in Fig. 4.

When there are two control parameters, systems can be classified into either a fold catastrophe or a cusp catastrophe. In the present case, since we find that the bifurcation set forms a curve without a cusp in Fig. 4, our model classified into a fold catastrophe which is the simplest but nontrivial case. A fold catastrophe needs only one control parameter essentially and the other control parameter becomes a dummy parameter which is not important for the catastrophe analysis.

In the stability analysis using catastrophe theory, we pay attention to certain modes of the system. In our case we consider only a spherically symmetric spacetime, hence, relevant modes must be restricted to radial ones. This will be confirmed in the next subsection. When we will analyze nonspherically symmetric modes, we may need a different approach.

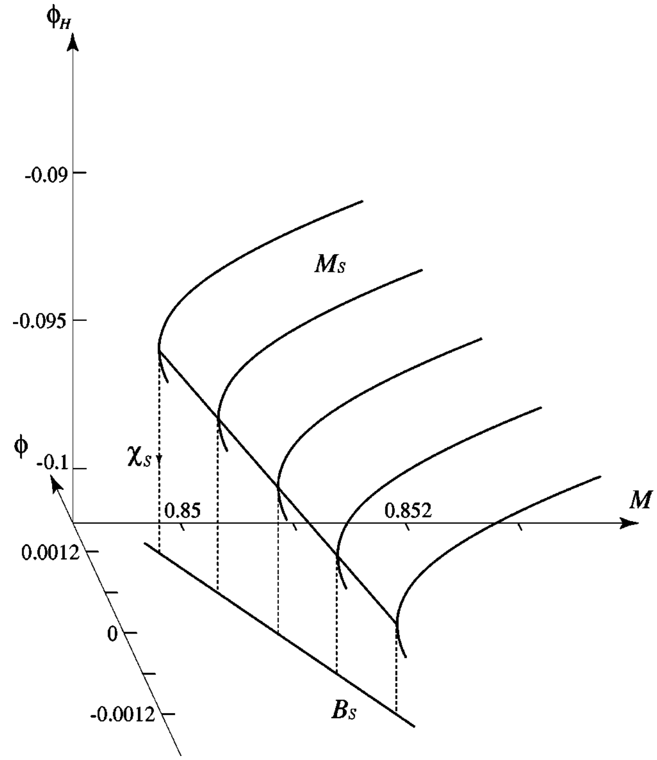

FIG. 4. The equilibrium space of the dilatonic black holes with Gauss-Bonnet term. Upper side and lower side of the equilibrium space correspond to the stable and unstable solutions, respectively. When the black hole mass gets small, the stable and the unstable solutions merge at a critical point. On the control plane, we draw the bifurcation set B_S, which shows a fold catastrophe.

B. Linear stability analysis

In order to confirm our results obtained by catastrophe theory that solutions in the upper branch are stable, we turn to a linear perturbation analysis. Here we focus only on the radial modes. First we expand field variables around a static solution as follows:

$$\phi(\tilde{r},\tilde{t}) = \phi_{(0)}(\tilde{r}) + \phi_{(1)}(\tilde{r},\tilde{t})\epsilon, \tag{34}$$

$$\Phi(\tilde{r},\tilde{t}) = \Phi_{(0)}(\tilde{r}) + \Phi_{(1)}(\tilde{r},\tilde{t})\epsilon, \tag{35}$$

$$\Lambda(\tilde{r},\tilde{t}) = \Lambda_{(0)}(\tilde{r}) + \Lambda_{(1)}(\tilde{r},\tilde{t})\epsilon, \tag{36}$$

here ϵ is an infinitesimal parameter. Substituting them into the field equations (10)–(14), and dropping the second- and higher-order terms of ϵ, we find the perturbation equation for the dilaton field ϕ, which is decoupled as

$$F_1\ddot{\phi}_{(1)} + F_2\phi''_{(1)} + F_3\phi'_{(1)} + F_4\phi_{(1)} = 0, \tag{37}$$

where F_i $(i=1\text{–}4)$ are complicated functions of zeroth order variables, whose explicit forms are given in the Appendix. Since Eq. (37) becomes singular on the event horizon, we introduce the tortoise coordinate $\tilde{r}^*$ defined by

$$\frac{d\tilde{r}^*}{d\tilde{r}} = e^{-(\Phi_{(0)}-\Lambda_{(0)})}. \tag{38}$$

To analyze the stability, we set $\phi_{(1)}$ as

$$\phi_{(1)}(\tilde{r},\tilde{t}) = \xi(\tilde{r}) e^{i\tilde{\sigma}\tilde{t}}. \tag{39}$$

If $\tilde{\sigma}$ is real, ϕ oscillates around the static solution and then the solution is stable. On the other hand, if the imaginary part of $\tilde{\sigma}$ is negative, the perturbation $\phi_{(1)}$ diverges exponentially with time and then the solution is unstable. With Eqs. (38) and (39), the perturbation equation becomes

$$\frac{d^2\xi}{d\tilde{r}^{*2}} + G_1 \frac{d\xi}{d\tilde{r}^*} + (G_2 - G_3\tilde{\sigma}^2)\xi = 0, \tag{40}$$

where

$$G_1 = e^{-(\Lambda_{(0)}-\Phi_{(0)})}\left((\Lambda'_{(0)} - \Phi'_{(0)}) + \frac{F_3}{F_2} \right), \tag{41}$$

$$G_2 = e^{-(2\Lambda_{(0)}-2\Phi_{(0)})}\frac{F_4}{F_2}, \tag{42}$$

$$G_3 = e^{-(2\Lambda_{(0)}-2\Phi_{(0)})}\frac{F_1}{F_2}. \tag{43}$$

Introducing a new function χ as

$$\chi(\tilde{r}^*) \equiv \xi(\tilde{r}^*) \exp\left(\int_{-\infty}^{\tilde{r}^*} \frac{G_1}{2} d\tilde{r}^* \right), \tag{44}$$

finally we obtain a simple form of the perturbation equation:

$$\frac{d^2\chi}{d\tilde{r}^{*2}} - (V_1 + V_2\tilde{\sigma}^2)\chi = 0, \tag{45}$$

where

$$V_1 = \frac{1}{2}\frac{dG_1}{d\tilde{r}^*} + \frac{{G_1}^2}{4} - G_2, \tag{46}$$

$$V_2 = G_3. \tag{47}$$

Equation (40) or Eq. (45) is a Strum-Liouville equation and σ^2 and ξ (or χ) are the eigenvalue and the eigenfunction, respectively. In a numerical calculation, we have solved Eq. (40) instead of Eq. (45) because the functions in Eq. (40) are much simpler and then it is easier to analyze it.

The eigenfunction must be finite in the whole region. This means $\xi \to 0$ $(\tilde{r}^* \to \pm\infty)$ for the eigenfunction with a negative eigenvalue. With this boundary condition, we have searched a negative eigenmode, and found it only in the lower branch in Fig. 3. We show the eigenvalue σ^2 and the eigenfunction ξ for several radii of event horizon in Figs. 5 and 6, respectively. Although the function ξ crosses at the same point $(\tilde{r}^* = 1.57)$, it does not have any physical meaning because we can shift ξ arbitrarily by changing an integral constant of the differential equation (38). Hence, these solutions are unstable against the radial perturbations. We could not find any unstable mode in the upper branch. We may

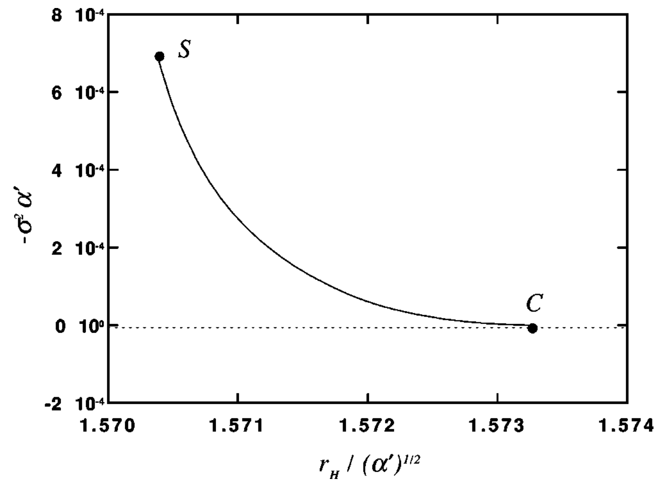

FIG. 5. The eigenvalue of the perturbation equation of the dilatonic black holes with Gauss-Bonnet term. For the lower branch of the M-S diagram, we found negative eigenvalues, which means that these solutions are unstable for radial perturbation. On the other hand, there is no negative eigenvalue for the upper branch. Since the eigenvalue becomes zero at the critical point, stability change occurs at this point. This result is consistent with that obtained by a catastrophe analysis.

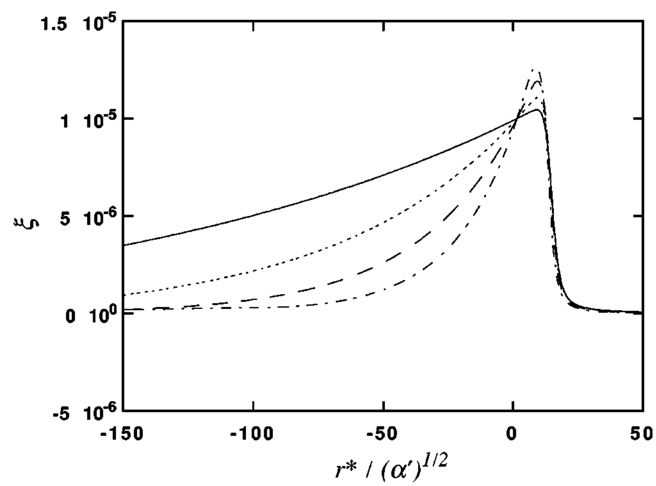

FIG. 6. We show the behavior of the eigenfunctions for the lower branch of M-r_H diagram. The radius of black holes are $r_H = 1.5724$ (solid line), $r_H = 1.5716$ (dotted line), $r_H = 1.5708$ (dashed line), $r_H = 1.5702$ (dot-dashed line). Although they cross at the same point $(r^* = 1.57)$, it does not have any physical meaning because we can shift eigenfunctions arbitrarily by changing an integral constant of Eq. (38).

conclude that the solutions in the upper branch are absolutely stable as we expected. The critical point C has eigenvalue zero. This means that a stability change occurs at this point. These results are exactly the same as those we showed by using catastrophe theory in the previous subsection.

C. Comment on the stability analysis by using Strum's theorem

Kanti *et al.* claimed that all black holes obtained here are stable using a semianalytic method or catastrophe theory [21]. We should comment on that. Their semianalytic method is as follows. They first derive the perturbation equation (45). Next they prepare two infinitesimally close static solutions, $\phi_1(r)$ and $\phi_2(r)$, which have the same horizon radius, but different asymptotic values of ϕ_∞. Since these functions satisfy the static equations, they claimed that the difference $\overline{\phi}_{(1)}=\phi_2-\phi_1$ satisfies the perturbation equation (45) with $\tilde{\sigma}^2=0$, i.e., $\overline{\phi}_{(1)}$ is one of the eigenfunctions with the eigenvalue 0. (This is not correct as we will show below.) Then they apply Strum's theorem, which says that if there exist eigenfunctions f_1 and f_2 with eigenvalues σ_1^2 and σ_2^2, respectively, such that $\sigma_1^2>\sigma_2^2$, then f_1 must have at least one node between any two nodes of f_2, if any. If a dilatonic black hole with Gauss-Bonnet term has an unstable mode, i.e., $\tilde{\sigma}^2<0$, the corresponding eigenfunction has ''nodes'' at $\tilde{r}^*=\pm\infty$. Strum's theorem demands the eigenfunction $\overline{\phi}_{(1)}$, whose eigenvalue is $\tilde{\sigma}^2=0$, must have at least one node somewhere in $(-\infty,\infty)$. However numerical calculation shows that any pair of $\phi_1(r)$ and $\phi_2(r)$ does not intersect anywhere, so the eigenfunction $\overline{\phi}_{(1)}$ is nodeless. This is inconsistent with saying that $\overline{\phi}_{(1)}$ has at least one node. As a result, Kanti *et al.* concluded that there is no unstable mode and *all* dilatonic black holes with Gauss-Bonnet term are stable.

Apparently, their results disagree with ours that the solutions of the lower branch in M-S diagram are unstable. The disagreement comes from the fact that they regard $\overline{\phi}_{(1)}$ as the solution of the perturbation equation (45) with $\tilde{\sigma}^2=0$. The perturbation equation (45) is derived by using the (t,r) component of the Einstein equation (A8) or (A41) (see the detail in Appendix). However, as $\overline{\phi}_{(1)}(r)$ (the difference of two static solutions) does not depend on $\tilde{t}$, Eq. (A8) becomes trivial. As a result, $\overline{\phi}_{(1)}(r)$ no longer satisfies the perturbation equation (45) with $\tilde{\sigma}^2=0$. In fact, it satisfies the *time-independent* perturbation equations:

$$\overline{F}_1\phi''_{(1)}+\overline{F}_2\phi'_{(1)}+\overline{F}_3\phi_{(1)}+\overline{F}_4\Lambda_{(1)}=0, \tag{48}$$

$$\Lambda'_{(1)}=\overline{G}_1\phi''_{(1)}+\overline{G}_2\phi'_{(1)}+\overline{G}_3\phi_{(1)}+\overline{G}_4\Lambda_{(1)}, \tag{49}$$

which are different from Eq. (45) with $\tilde{\sigma}^2=0$ (see Appendix). We have also checked numerically that $\overline{\phi}_{(1)}$ obtained by Eqs. (48) and (49) is really not the same as the eigenfunction of Eq. (45) with $\tilde{\sigma}^2=0$. Hence, we cannot use $\overline{\phi}_{(1)}$ in order to investigate the stability of our system by Strum's theorem.

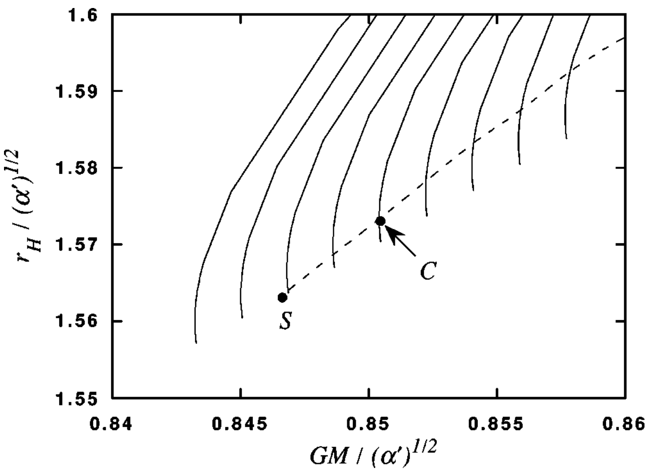

FIG. 7. The M-r_H diagram of the dilatonic black holes with Gauss-Bonnet term. Each solid line has the different boundary condition; $\phi_\infty=0.012$, 0.009, 0.006, 0.003, 0.0, -0.003, -0.006, -0.009, and -0.012 from the left side. We also plot the $\phi_H=-0.488$ line by a dotted line. We cannot find a turning point for dotted line, while there is a turning point for each solid line. However the dotted line passes through the turning point of the solid line and stability change occurs at this point.

Kanti *et al.* also used catastrophe theory. They showed a branch of static solutions with different boundary values of a dilaton field from ours. They have fixed ϕ on the event horizon and left that at infinity free, although we have fixed the value of ϕ at infinity and determined that on the event horizon to satisfy $\phi_\infty=0$. Then their M-r_H diagram does not show a turning point. Since their diagram is single valued with respect to M, no cusp structure appears even when we plot the M-S diagram with their boundary condition. As a result, they concluded that all solutions are stable.

What is the essential difference between their analysis and ours? In order to clarify this problem, we vary the ϕ_∞ and plot the M-r_H diagram in Fig. 7. Each branch is obtained by scaling from the original branch with $\phi_\infty=0$ because the changing of ϕ_∞ by a constant can be absorbed by normalization of r_H and M as we mentioned. As a result, each branch has a turning point in the M-r_H diagram and a cusp structure in the M-S diagram. We then trace the $\phi_H=$constant solutions as shown by dotted lines in Fig. 7. As we can see from Fig. 7, the $\phi_H=$constant curve can change monotonically without any cusp structure, although a cusp structure appears in any $\phi_\infty=$constant curves. The trick comes from that they fix the state variable, i.e., ϕ_H. It is shown that fixing the state variable can lead to a wrong result [15]. Therefore we believe that the solutions in a $\phi_H=$constant branch also become unstable beyond the point corresponding to our critical point C, although no cusp structure appears.

IV. CONCLUSION AND REMARKS

We have studied the stability of dilatonic black holes with the Gauss-Bonnet term. The minimum mass solution at the critical point divides them into two branches in the M-S diagram. The upper branch has the $r_H\to\infty$ limiting solution, which corresponds to a Schwarzschild black hole; on the other hand, the lower branch ends up with the singular point, where a naked singularity will appear. By catastrophe theory analysis, the solutions of upper branch are stable, while those in lower branch are found to be unstable. As catastrophe theory tells us, only relative stability between several families of solutions and we are not sure whether catastrophe theory is applicable for any generalized theory of gravity, we have also checked stability by linear perturbation analysis. Then we find one unstable mode in the lower branch, but no unstable mode in the upper branch. The solution which has eigenvalue zero coincides with the critical point. Hence, the stability changes at this critical point. These results are exactly the same as those obtained by a catastrophe theory analysis. Hence, our investigation gives one evidence that catastrophe theory is useful not only in general relativity, but also in the generalized theory of gravity [15].

The global structure of dilatonic black holes with Gauss-Bonnet term was studied by Alexeev and Pomazanov [8]. They found that a spacelike singularity extends at $r=r_s>0$ inside the event horizon. This global structure is almost the same as that of the Schwarzschild black hole. We find that the location of the singularity approaches the event horizon as the horizon radius gets smaller. Eventually, the singularity and the event horizon coincide at the singular point S. Thus a naked singularity appears at $r=r_s=r_H$. Can a naked singularity appear in the real universe? We could give an answer for this question. Suppose that a black hole in the lower branch is formed first. One may expect that as remaining matter around falls into a black hole, the spacetime evolves along the lower branch of M-S diagram to the singular point S and eventually a naked singularity appears. However, since the solutions in the lower branch are unstable as we showed, those jump up to the solution in the upper branch by some perturbations caused by matter accretion. There might be some initial data, which evolves into the singular solution S without forming an event horizon. However such a scenario seems unlikely because the singular solution S belongs to the unstable branch. As a result, the singular solution is not generically formed. This may support the cosmic censorship conjecture.

If we consider quantum mechanics, i.e., if we include an evaporation process, more careful treatment is required. Suppose the unstable black hole solution in the lower branch is formed. How does this black hole evolve? We have to compare two time scales; the time scale of instability t_{inst} and the evaporation time scale t_{evap}. As the eigenvalue of the linear perturbation equation is $\sigma^2 \sim 10^{-4}/\alpha'$, the time scale that instability grows is estimated as $t_{inst} \sim 100\sqrt{\alpha'}$. On the other hand, since the temperature of the black hole in the lower branch is $T \sim 0.05/\sqrt{\alpha'}$, the evaporation time scale from the singular point S to the critical point C is estimated as

$$t_{evap} \sim (M_s - M_c) \Big/ \left(\frac{\pi^2}{120} N T^4 \times A_{eff} \right) \sim 10 \frac{\sqrt{\alpha'}}{N g^2}, \quad (50)$$

where M_s and M_c are the masses of the black holes of the singular and the critical points, respectively [9], N is the number of evaporating particle species including spin weight, and $A_{eff} \sim O(10) \times A_H$ is the effective area of Hawking radiation [22]. Since the evaporation time scale is shorter than the instability time scale, the unstable solution will evaporate to the critical solution C before it jumps up into the stable upper branch. In any case, both stable and unstable solutions will evaporate into the critical solution C. After the spacetime reaches the critical point C, we are not sure what kind of state it evolves into.

We have to comment on the case with the gauge fields. In the electrically charged case, our results will be essentially the same as the present case. Since magnetically charged or ''colored'' black holes do not have a cusp in the M-S diagram, a black hole solution can evolve to a naked singularity via an evaporation process. In the ''colored'' case, we expect that sphaleron type instability of the Yang-Mills field [23] destroys such a solution and all solutions are unstable. However we have no idea about the magnetically charged black hole case. If it is stable, the cosmic censorship conjecture may not hold. Quantum gravity may play an essential and important role at the last stage.

Our results are obtained by assuming the model (1) which includes only the tree level of the leading order terms of the expansion parameter α'. There is a possibility that the solutions near the critical point and singular point may be modified by taking the one-loop quantum correction or next leading terms of α' into account. It is well known that the singularity theorem demands that the universe has an initial singularity in general relativity. According to the latest investigation of string cosmology, however, the moduli field with one-loop effect could remove an initial singularity and provide us a nonsingular cosmology [24,25]. Motivated by these discussions, we have studied the effect of the moduli field on the black hole solution as well. Preliminarily, we find that the properties of the solution are almost the same as the present model. In fact, the singular solution S appears at the end of branch in this case as well. The effect of the moduli field is not large enough to change the outside structure of the black hole, although an inside singularity might be removed. The detail will be discussed in a future publication.

ACKNOWLEDGMENTS

We would like to thank Paul Haines for his critical reading of our paper. This work was supported partially by the Grant-in-Aid for Scientific Research Fund of the Ministry of Education, Science and Culture (Specially Promoted Research No. 08102010), by the Grant-in-Aid (No. 094162), and by the Waseda University Grant for Special Research Projects.

APPENDIX: LINEAR PERTURBATION EQUATIONS

We show the explicit forms of the coefficients of linear perturbation equation (37). By using the time dependent expansions

$$\phi(\tilde{r},\tilde{t})=\phi_{(0)}(\tilde{r})+\phi_{(1)}(\tilde{r},\tilde{t})\epsilon, \tag{A1}$$

$$\Phi(\tilde{r},\tilde{t})=\Phi_{(0)}(\tilde{r})+\Phi_{(1)}(\tilde{r},\tilde{t})\epsilon, \tag{A2}$$

$$\Lambda(\tilde{r},\tilde{t})=\Lambda_{(0)}(\tilde{r})+\Lambda_{(1)}(\tilde{r},\tilde{t})\epsilon, \tag{A3}$$

we find the following first-order perturbation equations:

$$a_1\phi_{(1)}+a_2\phi'_{(1)}+\phi''_{(1)}+a_3\ddot{\phi}_{(1)}+a_4\Lambda_{(1)}+a_5\Phi'_{(1)}+a_6\Lambda'_{(1)}+a_7\Phi''_{(1)}+a_8\ddot{\Lambda}_{(1)}=0, \tag{A4}$$

$$\Phi''_{(1)}=b_1\phi_{(1)}+b_2\phi'_{(1)}+b_3\phi''_{(1)}+b_4\ddot{\phi}_{(1)}+b_5\ddot{\phi}'_{(1)}+b_6\Lambda_{(1)}+b_7\Lambda'_{(1)}+b_8D_{(1)}, \tag{A5}$$

$$\Lambda'_{(1)}=c_1\phi_{(1)}+c_2\phi'_{(1)}+c_3\phi''_{(1)}+c_4\Lambda_{(1)}+c_5D_{(1)}, \tag{A6}$$

$$\Phi'_{(1)}=d_1\phi'_{(1)}+d_2\ddot{\phi}_{(1)}+d_3\Lambda_{(1)}+d_4D_{(1)}, \tag{A7}$$

$$\dot{\Lambda}_{(1)}=e_1\dot{\phi}_{(1)}+e_2\dot{\phi}'_{(1)}, \tag{A8}$$

$$D_{(1)}=f_1\phi_{(1)}+f_2\phi'_{(1)}+f_3\Lambda_{(1)}, \tag{A9}$$

where coefficients are

$$a_1=\frac{8\gamma^2\tilde{f}_{(0)}}{\tilde{r}^2}[2\Lambda'_{(0)}\Phi'_{(0)}-(1-e^{-2\Lambda_{(0)}})(\Phi''_{(0)}-3\Lambda'_{(0)}\Phi'_{(0)}+\Phi'^{2}_{(0)})], \tag{A10}$$

$$a_2=-\Lambda'_{(0)}+\Phi'_{(0)}+\frac{2}{\tilde{r}}, \tag{A11}$$

$$a_3=-e^{2\Lambda_{(0)}-2\Phi_{(0)}}, \tag{A12}$$

$$a_4=\frac{16\gamma\tilde{f}_{(0)}}{e^{2\Lambda_{(0)}}\tilde{r}^2}(\Phi''_{(0)}-3\Lambda'_{(0)}\Phi'_{(0)}+\Phi'^{2}_{(0)}), \tag{A13}$$

$$a_5=\frac{1}{e^{2\Lambda_{(0)}}\tilde{r}^2}[8\gamma\tilde{f}_{(0)}(3\Lambda'_{(0)}-2\Phi'_{(0)}-\Lambda'_{(0)}e^{2\Lambda_{(0)}}+2\Phi'_{(0)}e^{2\Lambda_{(0)}})+\phi'_{(0)}e^{2\Lambda_{(0)}}\tilde{r}^2], \tag{A14}$$

$$a_6=-\phi'_{(0)}-\frac{8\gamma\tilde{f}_{(0)}\Phi'_{(0)}(1-3e^{-2\Lambda_{(0)}})}{\tilde{r}^2}, \tag{A15}$$

$$a_7=\frac{8\gamma\tilde{f}_{(0)}(1-e^{-2\Lambda_{(0)}})}{\tilde{r}^2}, \tag{A16}$$

$$a_8=\frac{8\gamma\tilde{f}_{(0)}e^{-2\Phi_{(0)}}(1-e^{2\Lambda_{(0)}})}{\tilde{r}^2}, \tag{A17}$$

$$b_1=\frac{\gamma^2\tilde{f}_{(0)}}{D_{(0)}^{2}\tilde{r}^3e^{2\Lambda_{(0)}}}[(3-e^{2\Lambda_{(0)}})(\phi'_{(0)}-\tilde{r}\phi''_{(0)}+\tilde{r}\gamma\phi'^{2}_{(0)})+6\Lambda'_{(0)}\phi'_{(0)}\tilde{r}](2-2e^{2\Lambda_{(0)}}-\phi'^{2}_{(0)}\tilde{r}^2), \tag{A18}$$

$$b_2 = \frac{1}{2D_{(0)}{}^2 e^{2\Lambda_{(0)}}\tilde{r}^3}[-4\gamma\tilde{f}_{(0)}(1+2\tilde{r}\gamma\phi'_{(0)})(1-e^{2\Lambda_{(0)}})(3-e^{2\Lambda_{(0)}})+D_{(0)}\tilde{r}^3 e^{2\Lambda_{(0)}}(\phi'_{(0)}+\tilde{r}\phi''_{(0)})$$
$$+2\tilde{r}^2\gamma\tilde{f}_{(0)}\phi'_{(0)}{}^2(3+4\tilde{r}\phi'_{(0)}\gamma)(3-e^{2\Lambda_{(0)}})-12\tilde{r}\Lambda'_{(0)}\gamma\tilde{f}_{(0)}(2-2e^{2\Lambda_{(0)}}-3\tilde{r}^2\gamma\phi'_{(0)}{}^2)$$
$$-4\phi'_{(0)}\phi''_{(0)}\gamma\tilde{r}^3\tilde{f}_{(0)}(4-e^{2\Lambda_{(0)}})], \tag{A19}$$

$$b_3 = \frac{1}{2D_{(0)}{}^2\tilde{r}^2 e^{2\Lambda_{(0)}}}[2\gamma\tilde{f}_{(0)}(3-4e^{2\Lambda_{(0)}})(2-2e^{2\Lambda_{(0)}}-\tilde{r}^2\phi'_{(0)}{}^2)+D_{(0)}\phi'_{(0)}e^{2\Lambda_{(0)}}\tilde{r}^3], \tag{A20}$$

$$b_4 = \frac{4\gamma\tilde{f}_{(0)}}{D_{(0)}{}^2 e^{2\Lambda_{(0)}}e^{2\Phi_{(0)}}\tilde{r}^3}\{4\gamma\tilde{f}_{(0)}(\phi'_{(0)}-\gamma\phi''_{(0)}+\tilde{r}\gamma\phi'_{(0)}{}^2)(1-e^{2\Lambda_{(0)}})(3-e^{2\Lambda_{(0)}})-\tilde{r}(1-e^{2\Lambda_{(0)}})$$
$$\times[D_{(0)}e^{2\Lambda_{(0)}}(1+2\tilde{r}\Phi'_{(0)}+\tilde{r}\gamma\phi'_{(0)})-24\tilde{r}\phi'_{(0)}\Lambda'_{(0)}\gamma\tilde{f}_{(0)}]-2D_{(0)}\Lambda'_{(0)}e^{4\Lambda_{(0)}}\tilde{r}^2\}, \tag{A21}$$

$$b_5 = \frac{4\gamma\tilde{f}_{(0)}(1-e^{2\Lambda_{(0)}})}{D_{(0)}\tilde{r}e^{2\Phi_{(0)}}}, \tag{A22}$$

$$b_6 = \frac{1}{D_{(0)}{}^2 e^{2\Lambda_{(0)}}\tilde{r}^3}[2\gamma\tilde{f}_{(0)}(\phi'_{(0)}-\tilde{r}\phi''_{(0)}+\tilde{r}\gamma\phi'_{(0)}{}^2)(6-2e^{4\Lambda_{(0)}}-3\tilde{r}^2\phi'_{(0)}{}^2)-D_{(0)}\tilde{r}e^{4\Lambda_{(0)}}(1-2\tilde{r}\Lambda'_{(0)})$$
$$+12\Lambda'_{(0)}\tilde{r}\gamma\phi'_{(0)}\tilde{f}_{(0)}(2-\tilde{r}^2\phi'_{(0)}{}^2)], \tag{A23}$$

$$b_7 = \frac{1}{D_{(0)}{}^2 e^{2\Lambda_{(0)}}\tilde{r}^2}[-6\gamma\phi'_{(0)}\tilde{f}_{(0)}(2-2e^{2\Lambda_{(0)}}-\tilde{r}^2\phi'_{(0)}{}^2)+D_{(0)}e^{4\Lambda_{(0)}}\tilde{r}], \tag{A24}$$

$$b_8 = \frac{1}{4\tilde{r}^3 D_{(0)}{}^3 e^{2\Lambda_{(0)}}}[8\gamma\tilde{f}_{(0)}(3-e^{2\Lambda_{(0)}})(2-2e^{2\Lambda_{(0)}}-\tilde{r}^2\phi'_{(0)}{}^2)(\phi'_{(0)}-\tilde{r}\phi''_{(0)}+\tilde{r}\gamma\phi'_{(0)}{}^2)$$
$$-\tilde{r}(D_{(0)}e^{2\Lambda_{(0)}}-48\Lambda'_{(0)}\gamma\phi'_{(0)}\tilde{f}_{(0)})(2-2e^{2\Lambda_{(0)}}-\tilde{r}^2\phi'_{(0)}{}^2)$$
$$-2D_{(0)}\tilde{r}^2 e^{2\Lambda_{(0)}}(2\Lambda'_{(0)}e^{2\Lambda_{(0)}}+\tilde{r}^2\phi'_{(0)}\phi''_{(0)}+\tilde{r}\phi'_{(0)}{}^2)], \tag{A25}$$

$$c_1 = \frac{4\gamma^2\tilde{f}_{(0)}}{D_{(0)}\tilde{r}}(1-e^{-2\Lambda_{(0)}})(\phi''_{(0)}-\phi'_{(0)}{}^2\gamma), \tag{A26}$$

$$c_2 = \frac{\phi'_{(0)}}{2D_{(0)}\tilde{r}}[16\gamma^2\tilde{f}_{(0)}(1-e^{-2\Lambda_{(0)}})+\tilde{r}^2], \tag{A27}$$

$$c_3 = \frac{-4\gamma\tilde{f}_{(0)}(1-e^{-2\Lambda_{(0)}})}{D_{(0)}\tilde{r}}, \tag{A28}$$

$$c_4 = \frac{1}{D_{(0)}\tilde{r}}[-e^{2\Lambda_{(0)}}-8\gamma\tilde{f}_{(0)}e^{-2\Lambda_{(0)}}(\phi''_{(0)}-\phi'_{(0)}{}^2\gamma)], \tag{A29}$$

$$c_5 = \frac{1}{4D_{(0)}{}^2\tilde{r}}[-2+2e^{2\Lambda_{(0)}}-\phi'_{(0)}{}^2\tilde{r}^2+16\gamma\tilde{f}_{(0)}(1-e^{-2\Lambda_{(0)}})(\phi''_{(0)}-\phi'_{(0)}{}^2\gamma)], \tag{A30}$$

$$d_1 = \frac{\tilde{r}\phi'_{(0)}}{2D_{(0)}}, \tag{A31}$$

$$d_2=\frac{4\gamma\tilde{f}_{(0)}(1-e^{2\Lambda_{(0)}})}{D_{(0)}\tilde{r}e^{2\Phi_{(0)}}}, \tag{A32}$$

$$d_3=\frac{e^{2\Lambda_{(0)}}}{D_{(0)}\tilde{r}}, \tag{A33}$$

$$d_4=\frac{2(1-e^{2\Lambda_{(0)}})-\phi_{(0)}'^{2}\tilde{r}^2}{4D_{(0)}{}^2\tilde{r}}, \tag{A34}$$

$$e_1=\frac{(1-e^{-2\Lambda_{(0)}})\{8\gamma\tilde{f}_{(0)}(\Phi'_{(0)}+\phi'_{(0)}\gamma)[(1-e^{2\Lambda_{(0)}})-2\tilde{r}(\Lambda'_{(0)}+\Phi'_{(0)})]-\phi'_{(0)}e^{2\Lambda_{(0)}}\tilde{r}^2\}}{2\tilde{r}[D_{(0)}(1-e^{2\Lambda_{(0)}})-2D_{(0)}\tilde{r}(\Lambda'_{(0)}+\Phi'_{(0)})+\phi_{(0)}'^{2}\tilde{r}^2]}, \tag{A35}$$

$$e_2=\frac{4\gamma\tilde{f}_{(0)}(1-e^{-2\Lambda_{(0)}})[-1+e^{2\Lambda_{(0)}}+2\tilde{r}(\Lambda'_{(0)}+\Phi'_{(0)})]}{\tilde{r}[D_{(0)}(1-e^{2\Lambda_{(0)}})-2D_{(0)}\tilde{r}(\Lambda'_{(0)}+\Phi'_{(0)})+\phi_{(0)}'^{2}\tilde{r}^2]}, \tag{A36}$$

$$f_1=\frac{4\phi'_{(0)}\gamma^2\tilde{f}_{(0)}(1-3e^{-2\Lambda_{(0)}})}{\tilde{r}}, \tag{A37}$$

$$f_2=\frac{4\gamma\tilde{f}_{(0)}(1-3e^{-2\Lambda_{(0)}})}{\tilde{r}}, \tag{A38}$$

$$f_3=\frac{-24\phi'_{(0)}\gamma\tilde{f}_{(0)}e^{-2\Lambda_{(0)}}}{\tilde{r}}, \tag{A39}$$

where

$$D_{(0)}=1+\frac{4}{\tilde{r}}\tilde{f}'_{(0)}(1-3e^{-2\Lambda_{(0)}}). \tag{A40}$$

Integrating Eq. (A8), we obtain

$$\Lambda_{(1)}=e_1\phi_{(1)}+e_2\phi'_{(1)}+\lambda_{(1)}(r), \tag{A41}$$

where $\lambda_{(1)}(r)$ is an arbitrary time-independent function. By differentiating Eq. (A41) with respect to r and by using zeroth- and other first-order equations, we find that $\lambda_{(1)}(r)$ satisfies the following differential equation:

$$\lambda'_{(1)}+\left(\Phi'_{(0)}-\Lambda'_{(0)}+\frac{1}{r}\right)\lambda_{(1)}=0. \tag{A42}$$

This is easily integrated as

$$\lambda_{(1)}=\frac{Ce^{\Lambda_{(0)}-\Phi_{(0)}}}{r}. \tag{A43}$$

C is an integration constant. Since $e^{\Lambda_{(0)}-\Phi_{(0)}}$ diverges on the event horizon, a regularity of perturbations forces $C=0$, i.e., $\lambda_{(1)}\equiv 0$. The same result can be easily obtained from Eq. (A8), when we set

$$\phi_{(1)}(\tilde{r},\tilde{t})=\xi(\tilde{r})e^{i\tilde{\sigma}\tilde{t}}, \tag{A44}$$

$$\Lambda_{(1)}(\tilde{r},\tilde{t})=\eta(\tilde{r})e^{i\tilde{\sigma}\tilde{t}}, \tag{A45}$$

for $\tilde{\sigma}\neq 0$.

From the above first-order equations (A4)–(A7), (A9), and (A41), we obtain the single perturbation equation of the dilaton field ϕ:

$$F_1\ddot{\phi}_{(1)}+F_2\phi''_{(1)}+F_3\phi'_{(1)}+F_4\phi_{(1)}=0, \tag{A46}$$

where F_i $(i=1\text{–}4)$ are some functions of zeroth-order variables defined by

$$F_1=a_3+a_7b_4+a_5d_2+a_8e_1, \tag{A47}$$

$$F_2=1+a_7b_3+a_6c_3+a_7b_7c_3, \tag{A48}$$

$$\begin{aligned}F_3=&a_2+a_7b_2+(a_6+a_7b_7)(c_2+c_4e_2)\\&+a_5d_1+(f_2+f_3e_2)(a_7b_8+a_6c_5+a_5d_4)\\&+a_7b_7(c_5f_2+c_5f_3e_2)+e_2(a_4+a_7b_6+a_5d_3),\end{aligned} \tag{A49}$$

$$\begin{aligned}F_4=&a_1+a_7b_1+(a_6+a_7b_7)(c_1+c_4e_1)\\&+(f_1+f_3e_1)(a_7b_8+a_6c_5+a_7b_7c_5+a_5d_4)\\&+e_1(a_4+a_8b_6+a_5d_3).\end{aligned} \tag{A50}$$

How about time-independent perturbations? In that case, we just find the perturbation equations (A4)–(A7), (A9) without time derivative terms. From those equations, we obtain

$$\overline{F}_1\phi''_{(1)}+\overline{F}_2\phi'_{(1)}+\overline{F}_3\phi_{(1)}+\overline{F}_4\Lambda_{(1)}=0, \tag{A51}$$

$$\Lambda'_{(1)}=\overline{G}_1\phi''_{(1)}+\overline{G}_2\phi'_{(1)}+\overline{G}_3\phi_{(1)}+\overline{G}_4\Lambda_{(1)}, \tag{A52}$$

where coefficients are

$$\overline{F}_1=1+a_7b_3+c_3(a_6+a_7b_7), \tag{A53}$$

$$\overline{F}_2=a_2+a_7b_2+(a_6+a_7b_7)(c_2+c_5f_2)+f_2(a_7b_8+a_5d_4)+a_5d_1, \tag{A54}$$

$$\overline{F}_3=a_1+a_7b_1+(a_6+a_7b_7)(c_1+c_5f_1)+f_1(a_7b_8+a_5d_4), \tag{A55}$$

$$\overline{F}_4=a_4+a_7b_6+(a_6+a_7b_7)(c_4+c_5f_3)+f_3(a_7b_8+a_5d_4)+a_5d_3, \tag{A56}$$

$$\overline{G}_1=c_3, \tag{A57}$$

$$\overline{G}_2=c_2+c_5f_2, \tag{A58}$$

$$\overline{G}_3=c_1+c_5f_1, \tag{A59}$$

$$\overline{G}_4=c_4+c_5f_3. \tag{A60}$$

Equations (A51) and (A52) cannot be reduced to a single equation with respect to the dilaton field because of the lack of an algebraic equation between $\phi_{(1)}$ and $\Lambda_{(1)}$ like Eq. (A41).

Notice that those equations for time-independent perturbations are not recovered from those for time-dependent perturbations by setting $\tilde{\sigma}=0$.

[1] G. W. Gibbons and K. Maeda, Nucl. Phys. **B298**, 741 (1988).
[2] D. Garfinkle, G. T. Horowitz, and A. Strominger, Phys. Rev. D **43**, 3140 (1991).
[3] D. G. Boulware and S. Deser, Phys. Lett. B **175**, 409 (1986).
[4] C. G. Callan, R. C. Myers, and M. J. Perry, Nucl. Phys. **B311**, 673 (1988/89).
[5] S. Mignemi and N. R. Stewart, Phys. Rev. D **47**, 5259 (1993); S. Mignemi, *ibid.* **51**, 934 (1995).
[6] B. A. Campbell, N. Kaloper, and K. A. Olive, Phys. Lett. B **285**, 199 (1992); B. A. Campbell, N. Kaloper, R. Madden, and K. A. Olive, Nucl. Phys. **B399**, 137 (1993).
[7] P. Kanti, N. E. Mavromatos, J. Rizos, K. Tamvalis, and E. Winstanley, Phys. Rev. D **54**, 5049 (1996).
[8] S. O. Alexeyev and M. V. Pomazanov, Phys. Rev. D **55**, 2110 (1997).
[9] T. Torii, H. Yajima, and K. Maeda, Phys. Rev. D **55**, 739 (1997).
[10] J. D. Bekenstein, Phys. Rev. D **5**, 1239 (1972); **5**, 2403 (1972); **51**, R6608 (1995).
[11] M. Heusler, J. Math. Phys. **33**, 3497 (1992).
[12] D. Sudarsky, Class. Quantum Grav. **12**, 579 (1995).
[13] K. Maeda, T. Tachizawa, T. Torii, and T. Maki, Phys. Rev. Lett. **72**, 450 (1994); T. Torii, K. Maeda, and T. Tachizawa, Phys. Rev. D **51**, 1510 (1995).
[14] T. Tachizawa, K. Maeda, and T. Torii, Phys. Rev. D **51**, 4054 (1995).
[15] T. Torii, K. Maeda, and T. Tamaki (unpublished).
[16] Another example is given in the paper by T. Tamaki, K. Maeda, and T. Torii, Phys. Rev. D **57**, 4870 (1998).
[17] D. Gross and J. H. Sloan, Nucl. Phys. **B291**, 41 (1987).
[18] G. Kang, Phys. Rev. D **54**, 7483 (1996).
[19] T. Jacobson and G. Kang, Phys. Rev. D **52**, 3518 (1995).
[20] R. M. Wald, Phys. Rev. D **48**, R3427 (1993); V. Iyer and R. M. Wald, *ibid.* **50**, 846 (1994).
[21] P. Kanti, N. E. Mavromatos, J. Rizos, K. Tamvakis, and E. Winstanley, Phys. Rev. D **57**, 6255 (1998).
[22] R. M. Wald, *General Relativity* (Chicago University Press, Chicago, 1984).
[23] O. Brodbeck and N. Straumann, Phys. Lett. B **324**, 309 (1994); P. Boschung *et al.*, Phys. Rev. D **50**, 3842 (1994); G. Lavrelashvili and D. Maison, Phys. Lett. B **343**, 214 (1995); M. Volkov, O. Brodbeck, G. Lavrelashvili, and N. Straumann, *ibid.* **349**, 438 (1995).
[24] I. Antoniadis, J. Rizos, and K. Tamvakis, Nucl. Phys. **B415**, 497 (1994).
[25] R. Easther and K. Maeda, Phys. Rev. D **54**, 7252 (1996).